(Received 12 April 2026, Accepted 22 May 2026, Scheduled 6 June 2026)

Gold Nanowire-Enhanced Quasi-D-Shaped SPR-PCF Biosensor for High-Sensitivity Phase-Matched Cancer Cell Detection

Prarthana Madhusoodanan, Neville Philips Jommy, Joel Tiji, Sangeetha Natarajan*, and Ashish Patwari

School of Electronics Engineering, Vellore Institute of Technology, Vellore 632014, Tamil Nadu, India

ABSTRACT: This paper presents a structurally optimized photonic crystal fiber (PCF) for a surface plasmon resonance (SPR) based biosensor, in which a gold nanowire is embedded within a U-shaped open microchannel to detect the presence of cancer cells. The proposed nanowire-based structure is capable of providing the localized enhancement of the electromagnetic field confinement and phase matching between the core mode and localized surface plasmon resonance (LSPR) compared to conventional thin-film SPR architectures. The given SPR-based PCF biosensor was mathematically studied using the finite element method (FEM) to optimize its performance within the near-infrared wavelength range. Systematic variation of parameters, such as nanowire diameter, air-hole diameter, number of air holes, and channel dimensions, optimized the sensor performance. The proposed sensor has a maximum wavelength sensitivity of 42,857 nm/RIU and an amplitude sensitivity of 189 RIU^{-1} within a range of refractive index 1.39–1.376 between healthy and cancer cells. The architecture has a higher confinement loss peak and good phase matching, which has proven to be superior to traditional thin-film configurations. The suggested SPR-based PCF biosensor can be a promising label-free and real-time biomedical diagnostic solution because of the relatively easy fabrication process, high mechanical strength, and high accuracy.

1. INTRODUCTION

Earlydetection of cancer significantly improves patient survival rates and reduces treatment complexity. Optical biosensors have emerged as powerful tools for label-free and real-time biomedical diagnostics owing to their high sensitivity to refractive index (RI) variations between healthy and malignant cells. Among these techniques, surface plasmon resonance (SPR) sensors have gained considerable attention because of their strong dependence on the dielectric permittivity changes at the metal–analyte interface.

Surface Plasmon Resonance (SPR) biosensors have been in the limelight in recent years due to their high sensitivity, real-time detection, and label-free operation. The incorporation of photonic crystal fibers (PCFs) has improved the performance of SPR biosensors, allowing strong interaction between light and matter. Many researchers have been working to improve the sensitivity, selectivity, and miniaturization of SPR biosensors using new geometric configurations. In recent times, researchers have been working on the utilization of PCF-SPR biosensors in cancer detection applications. A dual-sided polished PCF-SPR biosensor has been proposed, which has improved the efficiency of guided light coupled to the SPR modes, achieving high sensitivity values of over 22,000 nm/RIU for various types of cancer cell detection [1]. A dual-core dual-polished-PCF-SPR biosensor with high sensitivity performance, high wavelength sensitivity, and high resolution has also been proposed for accurate detection of cancer cells [2]. In another study, the authors proposed a PCF-SPR biosensor, which utilizes a bottom side polished PCF, achieving high sensitivity values of up to 25,000 nm/RIU, which emphasizes the importance of coatings in SPR biosensors [3].

Material engineering has played a crucial role in advancing SPR sensor performance. A hybrid structure incorporating gold, graphene, and $Ti_3C_2T_x$-MXene layers demonstrated significant improvement in sensitivity due to enhanced plasmonic coupling and biomolecule adsorption properties [4]. Similarly, black phosphorus has been employed as an additional plasmonic layer in slotted D-shaped PCF, thereby enhancing sensitivity in the detection of various cancerous cells [5]. Moreover, magnesium fluoride and graphene coatings have been employed to enhance sensitivity and amplitude, thus proving the effectiveness of multilayer configurations [6]. Furthermore, ultra-high sensitivity and stability have been obtained using silver plasmonic structures, along with protective TiO_2 coatings, thus preventing oxidation [7]. Geometrical variations in PCF configurations have been explored to enhance the performance of PCF sensors. A dual-channel D-shaped PCF-SPR sensor was employed to sense multiple analytes, thus proving the effectiveness of multi-channel configurations [8]. Similarly, a dual-core bilateral PCF-SPR biosensor was employed to enhance detection accuracy [9]. Moreover, bowtie-shaped PCF configurations have been employed, thus obtaining extremely high sensitivity values of 100,000 nm/RIU [10]. Furthermore, sensing ring configurations have been proposed to enhance evanescent interactions, thus reducing losses [11]. These configurations have been employed to sense biological samples, including blood components.

* Corresponding author: Sangeetha Natarajan (nsangeetha@vit.ac.in).

In addition to SPR-PCF, other photonic crystal structures have been used to develop biosensors for various applications. A photonic crystal-based microring resonator with topological edge states exhibited a high-quality factor and sensitivity in the detection of cancer cells. This indicates the potential of photonic crystal-based microring resonators in biosensing [12]. Moreover, terahertz PCF sensors with novel geometries have been used to develop biosensors with high relative sensitivity and low confinement loss for chemical detection. This indicates the potential of PCF sensors for biomedical diagnostics [13]. Recent developments have also focused on using intelligent techniques to improve biosensor performance. A machine learning-based SPR biosensor using a D-shaped dual-core PCF exhibited an accurate prediction of confinement loss. This indicates the potential of machine learning techniques for use in SPR biosensors [14]. Moreover, photonic crystal-based biosensors using emerging two-dimensional materials have been developed. These biosensors have the potential to develop next-generation biosensors using emerging two-dimensional materials such as graphene, MoS_2, and black phosphorus [15].

Comprehensive reviews of PCF-based SPR biosensors in biomedical applications have emphasized the importance of nanomaterials and structural optimization in achieving sensitivity and selectivity in biosensors [16]. Reviews of biosensors based on SPR for cancer biomarker detection have also emphasized the potential of biosensors for the early diagnosis of diseases, providing alternatives to conventional detection methods [17]. Gold-coated PCF biosensors for refractive index sensing have also been developed, providing exceptional sensitivity responses for biosensors [18]. Optimized biosensor designs considering structural parameters and feasibility have also been presented, confirming the importance of D-shaped PCF biosensors in providing linearity and applicability [19]. The literature also presents a clear perspective on the development and advancement of SPR-based PCF biosensors, confirming improvements in structural designs, materials, and hybrid sensing technologies [20].

Multiple designs of plasmonic structures have been investigated, such as nanowire and thin film plasmonics with a high wavelength sensitivity of 17,000 nm/RIU and a wide detection range. This shows that PCF-SPR sensors can be applied in high-end biomedical diagnostic systems, chemical sensors, and environmental monitoring [21]. PCF and SPR integration provides highly sensitive real-time and noninvasive cancer diagnosis with increased light-matter interaction that leads to a high level of performance, which has a wavelength sensitivity of 35,714 nm/RIU and amplitude sensitivity of $-1971\,\mathrm{RIU}^{-1}$ and has a strong potential for the early detection of cancer [22]. The design is simple to fabricate and improves analyte access and plasmonic coupling efficiency [23]. A dual-core PCF-SPR sensor has been proposed to detect human body fluids using refractive index changes, with a wavelength sensitivity of more than 12,000 nm/RIU [24].

There have been many improvements in optical biosensing technology that allow cancer biomarker detection through noninvasive and ultra-sensitive means, such as SPR, LSPR, fluorescence, and Raman sensors [25]. Moreover, the square-geometry PCF-SPR sensor with Au–TiO_2 interface material proved increased plasmon coupling and refractive index sensitivity [26]. There is another PCF-SPR sensor which was inspired by the Kagome structure to detect biomarkers with wavelength sensitivity of 18,900 nm/RIU [27]. It should be noted that reviews on PCF-SPR biosensors reveal the remarkable advances in the field [28]. Still, there are some obstacles regarding the development of compact, inexpensive, and ultrahigh-sensitivity SPR biosensors able to discriminate multiple cancer cells accurately. That is why it is critically important to create PCF-SPR biosensors with optimal geometries and materials.

A D-shaped PCF-SPR biosensor consisting of a PMMA-Au hybrid structure capable of detecting cancer with an unprecedented wavelength sensitivity of 31,000 nm/RIU with excellent polarization sensitivity has been proposed recently. It is evident from this study that proper structural parameters in combination with optimized plasmonic thickness contribute greatly to accurate refractive index sensing for cancer biomarkers [29]. A slotted D-shaped PCF-SPR biosensor with black phosphorus has been proposed in [15] for detecting cancerous cells. This biosensor is designed with multiple plasmonic layers, including Au, TiO_2, and black phosphorus, in order to increase light-matter interaction. It operates by measuring the difference in refractive index between healthy and cancerous cells. Resonance wavelength shift is used to sense cells in the process. The maximum wavelength sensitivity for MCF-7 breast cancer cells is reported as 11,429 nm/RIU. Additionally, optimization of structural parameters, including metal thickness, air holes, and plasmonic layers, has been shown in this work.

Moreover, the utilization of black phosphorus as another plasmonic medium led to better field confinement and higher sensitivity of the sensor. In this regard, a machine-learning-enhanced D-shape dual-core PCF-SPR sensor was suggested in [13]. The sensing characteristics of the mentioned sensor were studied through wavelength and amplitude interrogation approaches. In this way, a sensitivity of 16,000 nm/RIU for wavelength sensing and 765.21 RIU^{-1} for amplitude interrogation were obtained with respect to an analyte refractive index of 1.38. Dual-core structure was effective for enhancing mode coupling among the core modes and surface plasmon modes. Besides, by designing a new ANN model, the loss of confinement was predicted with a mean square error of 3.5363×10^{-6}. Recent studies have demonstrated advanced SPR-based sensing strategies for multi-analyte detection. For instance, a triple-channel SPR fiber sensor utilizing MoS_2-tuned resonance bands and ion-imprinted layers enabled simultaneous and selective detection of multiple heavy metal ions despite minimal refractive index differences [30]. Another study reports a TiO_2-assisted parallel SPR sensing platform capable of simultaneous refractive index and temperature measurement with improved sensitivity in the near-infrared regime [31].

Inherent problems with SPR-PCF biosensors include complicated manufacturing processes and instability caused by metal film layers. To overcome the limitations in current biosensors, a novel design of a U-shaped PCF sensor integrated with Au nanowire is introduced in this study, which helps improve the

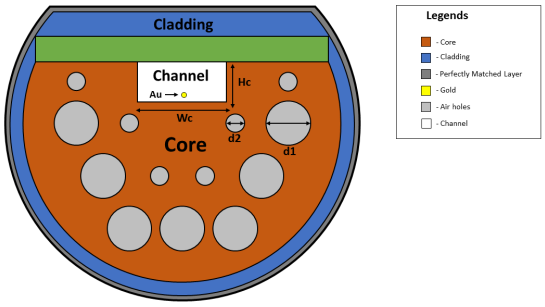

FIGURE 1. Two-dimensional cross-sectional view of the proposed quasi D-shaped PCF biosensor with embedded gold nanowire.

field localization and phase matching between the core waveguide mode and plasmonic modes.

2. SENSOR DESIGN AND THEORETICAL MODELING

The proposed biosensor is based on a photonic crystal fiber (PCF) designed by integrating a U-shaped open microchannel with a gold nanowire to excite surface plasmon resonance (SPR), as shown in Fig. 1. The background material of the proposed PCF is silica (SiO_2), whereas the cladding material is a hexagonal lattice of air holes. The central air hole was removed in this proposed PCF, resulting in a solid core suitable for efficient mode propagation. The air holes have respective diameters $d1$ and $d2$, pitch Λ, which are important parameters for effective refractive indices in this proposed PCF. The proposed gold nanowire is of diameter D_g, which is located inside this microchannel for an effective phase matching between the core mode of the proposed PCF and the LSPR mode. The proposed structure is effective in improving localized electromagnetic field confinement. The structural parameters used in the proposed quasi D-shaped SPR-PCF sensor are listed in Table 1.

2.1. Material Modeling and Numerical Method

The refractive index of silica is modeled using the Sellmeier equation:

$$n^2_{SiO_2}(\lambda) = 1 + \sum_{i=1}^{3} \frac{B_i \lambda^2}{\lambda^2 - C_i} \tag{1}$$

where λ represents the wavelength in µm. Equation (1) is used in the COMSOL simulation to accurately model the wavelength-dependent refractive index of the silica background material.

The dielectric function of gold was described using the Drude–Lorentz model:

$$\varepsilon_{Au}(\omega) = \varepsilon_\infty - \frac{\omega_D^2}{\omega(\omega + j\gamma_D)} - \frac{\Delta\varepsilon\Omega_L^2}{(\omega^2 - \Omega_L^2) + j\Gamma_L\omega} \tag{2}$$

Equation (2) is used to define the frequency-dependent permittivity of the gold nanowire, which is essential for accurately modeling surface plasmon resonance behavior in the proposed sensor.

The finite element method (FEM) of COMSOL Multiphysics was used to analyze the electromagnetic behavior of the sensor.

TABLE 1. Structural parameters of the proposed quasi D-shaped SPR-PCF sensor.

Parameter	Description	Value
Λ	Pitch (air-hole spacing)	4.5 µm
d_1	Large air hole diameter	3.8 µm
d_2	Small air hole diameter	0.16 µm
W_c	Channel width	8 µm
H_c	Channel depth	3.6 µm
D_g	Gold nanowire diameter	0.4 µm
R_a	Analyte region radius	13.5 µm
R_p	PML radius	14.5 µm

A perfectly matched layer (PML) is applied at the outer boundary to absorb outgoing radiation and eliminate back reflections. A very fine triangular mesh was employed, particularly around the nanowire and microchannel regions, to ensure numerical accuracy and convergence.

2.2. Performance Parameters and Optimization

The sensing performance was evaluated based on the confinement loss (CL), wavelength sensitivity, amplitude sensitivity, and resolution. The confinement loss is obtained from the imaginary part of the effective refractive index as follows:

$$CL\,(dB/cm) = 8.686 \times \frac{2\pi}{\lambda} \times \mathrm{Im}(n_{eff}) \times 10^4 \tag{3}$$

Equation (3) is used to compute the confinement loss spectrum from the simulated effective refractive index, and the resonance peak in this spectrum is used to identify phase-matching conditions.

Wavelength sensitivity is defined as:

$$S_\lambda = \frac{\Delta\lambda_{peak}}{\Delta n_a} \tag{4}$$

Equation (4) is used to quantify the shift in resonance wavelength corresponding to changes in analyte refractive index, which is obtained from the confinement loss spectra.

Amplitude sensitivity is expressed as:

$$S_A = -\frac{1}{CL(\lambda, n_a)} \frac{\partial CL(\lambda, n_a)}{\partial n_a} \tag{5}$$

Equation (5) evaluates the variation in confinement loss with respect to refractive index changes and is used to assess the sensor's response in amplitude interrogation mode.

The refractive index values of various normal and cancerous cells used in this study are summarized in Table 2. These values form the basis for evaluating the sensor's performance in distinguishing between healthy and malignant biological samples.

The confinement loss obtained using Equation (3) is analyzed for different parameter values to determine resonance behavior. The optimal design is selected based on maximum wavelength sensitivity (Equation (4)), sharp confinement loss

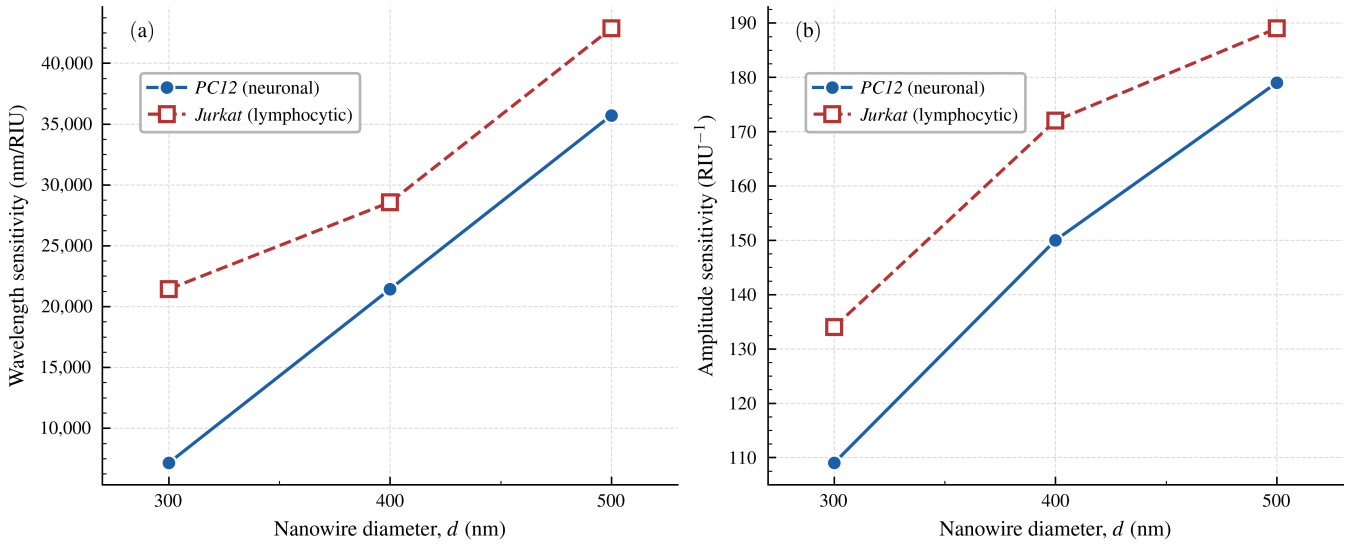

FIGURE 2. Variation of sensor performance with nanowire diameter for PC12 (neuronal) and Jurkat (lymphocytic) cancer cells: (a) wavelength sensitivity and (b) amplitude sensitivity, demonstrating enhanced sensing performance with increasing nanowire diameter.

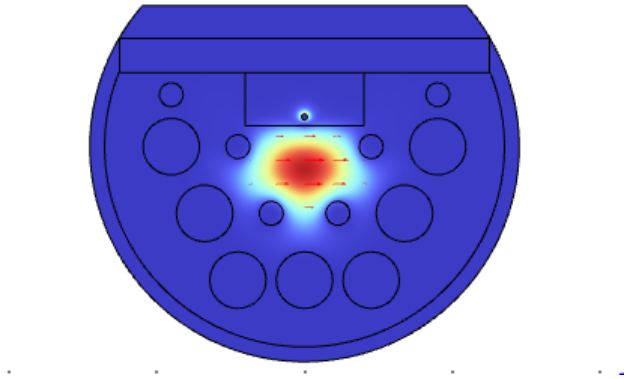

FIGURE 3. Electric field distribution of the core-guided mode at resonance.

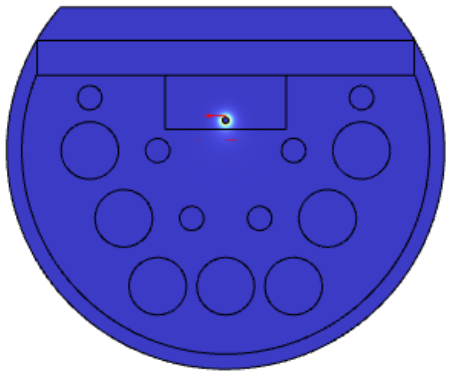

FIGURE 4. Electric field distribution of the localized surface plasmon resonance (LSPR) mode at the metal–analyte interface.

TABLE 2. Comparison of refractive indices between normal and cancer cells.

Name_Cell	Type and Concentration (%)	Refractive Index
Jurkat	Blood Cancer (80%)	1.390
	Normal Cell (30–70%)	1.376
HeLa	Cervical Cancer (80%)	1.392
	Normal Cell (30–70%)	1.368
PC-12	Adrenal Gland Cancer (80%)	1.395
	Normal Cell (30–70%)	1.381
MDA-MB-231	Breast Cancer (80%)	1.399
	Normal Cell (30–70%)	1.385
MCF-7	Breast Cancer (80%)	1.401
	Normal Cell (30–70%)	1.387
Basal	Skin Cancer (80%)	1.380
	Normal Cell (30–70%)	1.360

peaks, and increased amplitude sensitivity (Equation (5)). Additionally, as shown in Fig. 2 (sensitivity plots), both wavelength and amplitude sensitivities increase with nanowire diameter for PC12 and Jurkat cells, confirming that larger diameters improve sensing performance. The combined observations from these figures demonstrate that nanowire diameter plays a critical role in tuning resonance characteristics and enhancing the detection capability of the SPR-PCF biosensor.

The mode field distributions shown in Figs. 3 and 4 clearly demonstrate a strong phase matching between the guided mode and localized field mode at the resonant wavelength. The significant mode-field concentration near the surface of the nanowire clearly demonstrates efficient plasmon excitation.

The selection of the near-infrared (NIR) wavelength range is made due to beneficial features in terms of optics and biology. With respect to biology, in that wavelength range, there is lower absorption and scattering in biological samples, allowing deeper penetration of the evanescent field in the analyte sample. Moreover, gold shows better plasmonic properties in the near-infrared wavelength range; therefore, damping loss effects

in such structures are lower. Such features result in better phase matching in between the core guided mode and the LSPR mode, and thus higher wavelength sensitivity and resolution. Thus, the use of the NIR region helps greatly increase the sensitivity of the proposed biosensor to detect cancer cells.

In terms of structure fabrication, the proposed scheme eliminates difficulties related to multilayer fabrication and the photonic crystal drilling process. The U-shaped channel may be obtained using chemical etching or polishing processes in combination with traditional methods of depositing gold film on the structure (sputtering or evaporation).

2.3. Fabrication Feasibility

Nanowire alignment tolerance plays a crucial role in determining sensor effectiveness. A small lateral shift on the order of tens to hundreds of nanometers may have an impact on phase-matching criteria and mode coupling between the core mode and the localized mode. While the proposed gold nanowire-integrated U-shaped SPR-PCF biosensor structure exhibits many structural benefits over traditional thin-film sensors, actual fabrication raises some significant difficulties. Unlike metal films, nanowire alignment within the microchannel demands high-resolution micro-assembly technologies. The core PCF structure can be easily realized by employing the well-known stack-and-draw method, which can form predefined air holes and larger channels with a high degree of geometrical precision [21]. Moreover, the microchannel adjacent to the fiber core can be created utilizing modern micromachining techniques, such as focused ion beam (FIB) milling and femtosecond laser ablation, which are capable of submicron channel patterning and positioning accuracy [23].

The introduction of plasmonic nanowire may be considered from several points of view. In some cases, the insertion of nanowire in an open hole of larger size may be achieved by self-assembly caused by gravitational or capillary forces. For the case of the U-shaped channel configuration, micromanipulation or micro-positioning may be necessary. It should be noted that the problem of maintaining uniform alignment of one nanowire over long fiber lengths may present itself during experiments. This may result in positional errors, which might negatively influence the sensitivity of such a configuration due to phase mismatch and field overlap changes. Nevertheless, the use of the proposed method may provide more benefits than its conventional film analogues due to reduced nonuniform coating thickness, roughness, or delamination [22]. Consequently, while the procedure cannot be considered simple, recent advances in micromanipulation techniques indicate that the proposed structure can be implemented.

Although the above-described nanowire configuration brings along certain problems concerning its manufacturing process, it allows reaching a compromise between improved sensing properties and increased fabrication difficulty, thus making it useful in those cases where the priority lies not in large-scale production but rather in superior sensing capabilities. One of the most important practical questions concerning the aforementioned system relates to the stability of the nanowire inside the channel. Due to the difference between the size of the channel itself and the nanowire, there will inevitably arise a need for the latter's mechanical stabilization and adhesion. This can be done using such methods as thiol modification of the gold surface in order to secure chemically reliable bonds. It is also possible to anchor the nanowire partially or fully on the channel boundaries during the process of fabrication. From the point of view of fluid dynamics, the flow inside the microchannel should have a laminar regime due to the low Reynolds number characteristic of microscale structures, thus providing minimum perturbation effects on the nanowire. It is also possible to use such methods as polymer-mediated fixation, capillary-based alignment, or dielectric confinement.

3. RESULTS AND DISCUSSION

After optimizing the structural parameters, the sensor performance was evaluated within the refractive index (RI) range of 1.36–1.401, corresponding to various healthy and cancerous cells. The analysis was performed in the near-infrared wavelength region using the finite element method.

3.1. Confinement Loss Analysis

The confinement loss of the proposed SPR-PCF biosensor was examined to confirm that the resonant condition between the core and LSPR modes was satisfied. The confinement loss was caused by the conversion of the light intensity between the core mode and SPP mode of the gold nanowire at the metal-analyte interface. When the wavelength is increased, the effective refractive indices of both the core and SPP modes are similar. This causes a sharp peak in the loss spectrum, indicating that strong coupling between the two modes is taking place. This indicates a strong interaction between the surface plasmons and the evanescent field. The proposed nanowire structure is effective in creating a sharp peak in the loss spectrum owing to the higher localization of the electromagnetic field around the cylindrical surface of the gold nanowire, as shown in Fig. 5. This is due to its ability to detect changes in the refractive indices of biological fluids, including cancer cells, as shown in Fig. 6. The confinement loss spectrum was calculated using Equation (3) based on the imaginary part of the effective refractive index obtained from FEM simulations. As shown in Figs. 7–10, a distinct loss peak is observed, indicating strong phase matching between the core-guided mode and the plasmonic mode. The position of this peak is used to determine the resonance wavelength.

3.2. Sensitivity

The wavelength sensitivity is calculated using:

$$S_\lambda = \frac{\Delta\lambda_{peak}}{\Delta n_a} \tag{6}$$

The proposed nanowire-based sensor achieved a maximum wavelength sensitivity of 35,714 nm/RIU for PC12 cells and 42,857 nm/RIU for Jurkat cells, respectively. The high sensitivity is attributed to the improved electromagnetic field confinement and enhanced phase-matching efficiency enabled by the

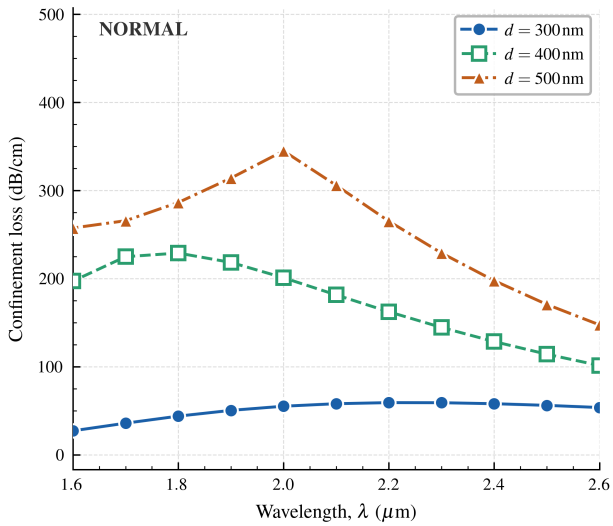

FIGURE 5. Confinement loss variation as a function of wavelength for normal cells at different nanowire diameters ($d = 300$ nm, 400 nm, and 500 nm).

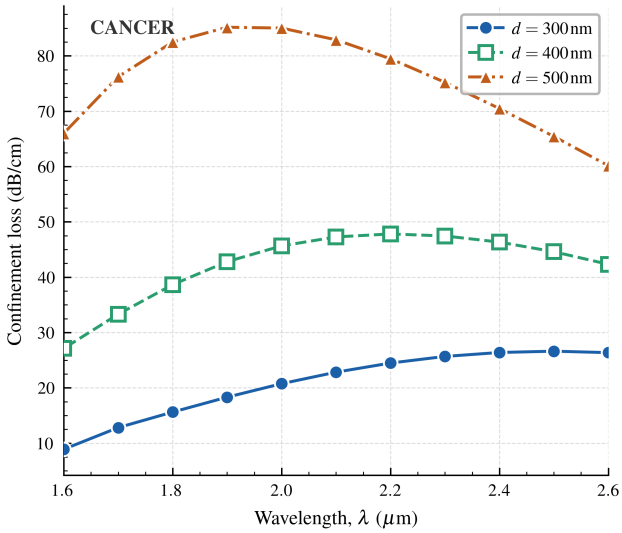

FIGURE 6. Confinement loss variation as a function of wavelength for cancerous cells at different nanowire diameters ($d = 300$ nm, 400 nm, and 500 nm).

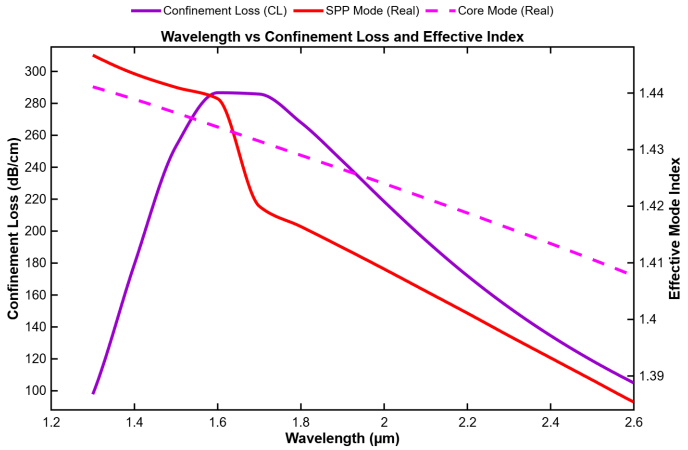

FIGURE 7. PC12 normal-cell-type phase-matching condition observed in the biosensor (nanowire diameter 0.5 μm).

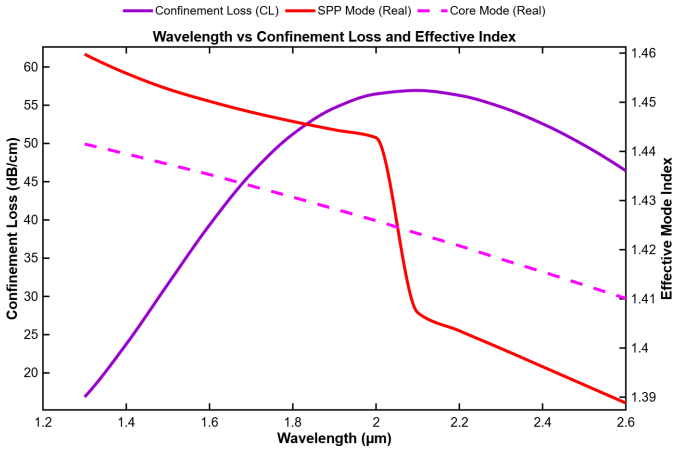

FIGURE 8. PC12 cancer-cell-type phase-matching condition observed in the biosensor (nanowire diameter 0.5 μm).

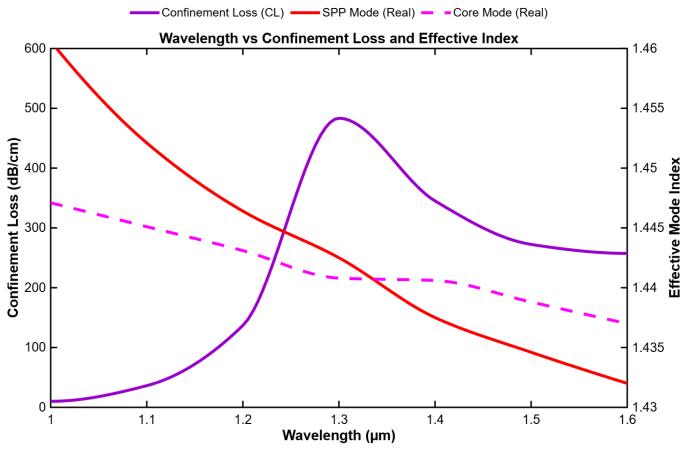

FIGURE 9. Jurkat normal-cell-type phase-matching condition observed in the biosensor (nanowire diameter 0.5 μm).

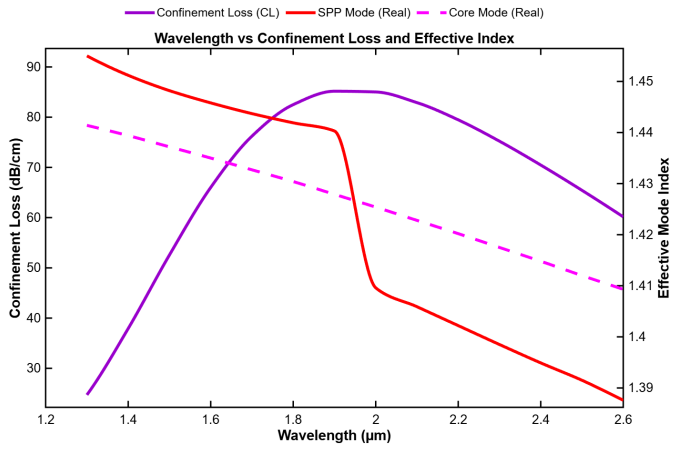

FIGURE 10. Jurkat cancer-cell-type phase-matching condition observed in the biosensor (nanowire diameter 0.5 μm).

gold nanowire geometry. The wavelength sensitivity was evaluated using Equation (4) by measuring the shift in resonance wavelength corresponding to changes in analyte refractive index. From Fig. 9 and Fig. 10, the resonance wavelength shifts from 1.3λ to 1.9λ as the refractive index increases, resulting in a maximum sensitivity of 42,857 nm/RIU.

The amplitude sensitivity is determined from the variation in the confinement loss with respect to the RI change as follows:

$$S_A = -\frac{1}{CL}\frac{\partial CL}{\partial n_a} \tag{7}$$

The maximum amplitude sensitivity obtained was 189 RIU^{-1}. The sharper resonance peak observed in the nanowire structure resulted in an improved amplitude interrogation performance. The amplitude sensitivity was calculated using Equation (5), which relates the variation in confinement loss to changes in analyte refractive index. As observed in Figs. 7–10, sharper confinement loss peaks lead to higher amplitude sensitivity values, confirming improved detection performance. The effect of structural parameters on sensor performance was analyzed by evaluating confinement loss using Equation (3) for different values of nanowire diameter and channel dimensions. The optimal configuration was selected based on maximum wavelength sensitivity (Equation (4)) and enhanced amplitude response (Equation (5)).

Recent advancements in PCF-SPR biosensors have demonstrated significant improvements in cancer cell detection using structural and material optimization techniques. A dual-core bilateral surface-optimized PCF-SPR biosensor achieved a wavelength sensitivity of 5714.28 nm/RIU for multiple cancer cell types [3]. Similarly, a black phosphorus-based slotted D-shaped PCF-SPR sensor exhibited an enhanced sensitivity of 11,429 nm/RIU for breast cancer detection [6]. In another approach, a machine learning-assisted dual-core D-shaped PCF-SPR sensor attained a sensitivity of 16,000 nm/RIU while improving prediction accuracy through ANN-based modeling [8]. Furthermore, a dual-core, dual-polished PCF-SPR biosensor demonstrated a maximum sensitivity of 7143 nm/RIU with an improved amplitude response and compact design [13]. In addition, hybrid material-based designs, such as gold/graphene/$Ti_3C_2T_x$-MXene coated D-shaped PCF-SPR sensors, achieved sensitivities of up to 9286 nm/RIU by enhancing plasmonic interactions through multilayer structures [19].

In contrast to these existing approaches, the proposed gold nanowire-integrated U-shaped PCF-SPR biosensor exhibited a significantly higher wavelength sensitivity of 42,857 nm/RIU. This substantial improvement is attributed to the strong localized surface plasmon resonance and enhanced electromagnetic field confinement induced by the nanowire geometry, which enable more efficient light–matter interactions and improved phase-matching conditions. Moreover, unlike hybrid material or machine-learning-based methods, the proposed design achieves superior performance through structural optimization alone, offering a simpler, more practical, and highly effective sensing solution.

3.3. Phase Matching Mechanism in the Proposed Geometry

The proposed quasi-D-shaped PCF structure allows for the efficient excitation of surface plasmon resonance by controlling the interaction between the evanescent field and the plasmonic nanowire. The fundamental core-guided mode propagates within the central defect region formed by removing the innermost air hole. The proximity of the microchannel to the core allows the evanescent field to interact strongly with the analyte-filled region containing gold nanowires.

The phase-matching condition is achieved when the propagation constant of the guided mode is equal to that of the surface plasmon polariton (SPP) mode:

$$\beta_{core} = \beta_{SPP} \tag{8}$$

Since $\beta = k_0 n_{eff}$, the resonance condition can be expressed as:

$$Re(n_{eff}^{core}) \approx Re(n_{eff}^{plasmon}) \tag{9}$$

Equations (8) and (9) define the phase-matching condition used in this work. This condition is verified in Figs. 7–10, where the effective indices of the core mode and SPP mode intersect at the resonance wavelength. At this point, maximum energy transfer occurs from the guided mode to the plasmonic mode, resulting in a sharp peak in the confinement loss spectrum. It is crucial to draw the distinction between the surface plasmon polariton (SPP) and the localized surface plasmon resonance (LSPR). In the traditional thin-film SPR system, SPPs constitute propagating electromagnetic waves that exist at the metal-dielectric interface with a definite propagation constant. On the other hand, the present structure contains a gold nanowire that supports LSPR, which consists of an electromagnetic field being confined to the metal surface but not propagating. This means that the sensing scheme in this case arises from the interactions of the guided mode in the core and the LSPR, which can be seen through the strong coupling, resulting in a loss peak. The strong coupling is further confirmed by the mode field distributions shown in Figs. 7–10, where the electromagnetic field initially concentrated in the core is redistributed toward the nanowire region at resonance. The cylindrical nanowire supports localized surface plasmon resonance (LSPR), which differs from planar SPR in thin-film configurations. Due to curvature, surface charges accumulate more strongly on the nanowire, enhancing the electric field intensity.

This can be explained using the electromagnetic boundary condition:

$$\varepsilon_m E_{m,\perp} = \varepsilon_a E_{a,\perp} \tag{10}$$

Equation (10) explains the field enhancement at the metal–dielectric interface. The curvature of the nanowire increases the normal electric field component, leading to stronger field localization around the nanowire surface. This enhanced localization improves the modal overlap between the guided mode and plasmonic mode, thereby strengthening the phase-matching condition defined in Equations (8) and (9).

As a result, sharper confinement loss peaks and higher wavelength shifts are observed, which directly contribute to improved amplitude and wavelength sensitivity in the proposed sensor.

TABLE 3. Performance comparison with existing PCF-SPR biosensors.

Ref	Year	Structure	Material	Sensitivity (nm/RIU)	Key Feature
[22]	2024	Nanowire infused square-clad PCF	Au	35714.28	Ultra-high dual sensitivity
[23]	2025	Nanowire Enhanced PCF	BP + Au	7857.14	Detection of 6 types of cancer
[26]	2025	Square PCF	Au + TiO_2	15,800	Integration of AI
[29]	2025	Quasi-D-Shaped	Au + PMMA	31,000	Cancer cell detection
[15]	2024	D-Shaped PCF	Au + TiO_2 + BP	11,429	Cancer cell detection
This Work	2026	**Quasi D-shaped PCF (nanowire)**	**Au NW**	**42,857**	**Localized SPR**

3.4. Comparison with Already Existing Works

Table 3 shows the comparison between the proposed biosensor and recently developed PCF-SPR biosensors. From Table 3, it can be observed that the proposed quasi-D-shaped biosensor containing the U-shaped channel embedded with gold nanowire exhibits substantially higher wavelength sensitivity than thin film biosensors and biosensors with hybrid materials. This is due to the localized surface plasmon resonance effect and electromagnetic field confinement provided by AuNWs. Moreover, the proposed biosensor is highly competitive in terms of wavelength sensitivity and works within a bio-friendly refractive index range.

3.5. Sensitivity Analysis for Cancer Cells

The sensing performance of the proposed biosensor was evaluated for PC12 and Jurkat cancer cells within their respective refractive index ranges. As shown in Table 4, the sensor exhibited high wavelength sensitivity values of 35,714 nm/RIU for PC12 cells and 42,857 nm/RIU for Jurkat cells. The enhanced sensitivity can be attributed to the strong phase-matching interaction between the core-guided mode and LSPR mode facilitated by the gold nanowire structure. Unlike conventional thin-film configurations, nanowires provide highly localized electromagnetic field confinement, resulting in stronger coupling and sharper resonance peaks. Furthermore, the U-shaped microchannel geometry allows the analyte to interact more effectively with the evanescent field, thereby increasing the overlap between the optical field and the sensing region. This leads to a more pronounced shift in the resonance wavelength for small changes in the refractive index. The higher sensitivity observed in Jurkat cells than PC12 cells is primarily due to the variation in the refractive index contrast, which affects the phase-matching condition and results in a larger resonance wavelength shift. Additionally, the relatively sharp confinement loss peaks obtained in the nanowire-based design contribute to improved amplitude sensitivity values of 175 RIU^{-1} for PC12 and 189 RIU^{-1} for Jurkat cells. These results demonstrate that the proposed nanowire-based SPR-PCF sensor significantly enhances sensing performance by improving the plasmonic coupling efficiency and field localization, making it suitable for high-precision cancer detection applications.

TABLE 4. Effect of nanowire diameter on sensor performance.

Cell Type	D_g (μm)	WS (nm/RIU)	AS (RIU^{-1})
PC12	0.3	7142	109
PC12	0.4	21428	150
PC12	0.5	35714	175
Jurkat	0.3	21428	134
Jurkat	0.4	28571	172
Jurkat	0.5	42857	189

3.6. Discussion on Biological Modeling Assumptions

In this work, cancer cells are described by the effective refractive index (1.36–1.401) interval. Such an approach is often applied in SP biosensing while modeling the refractive index of cell suspensions, biofluids, or their lysates, since it takes into account not the optical properties of single cells but averaged values. Indeed, biological cells are nonuniform objects containing numerous organelles, such as the nucleus and cytoplasm, which result in spatial refractive index variation inside the cell. Moreover, the cell size can lead to scattering phenomena when it interacts with an optical field. Nevertheless, as in the case of other sensors based on SPR-PCF, interaction occurs via the evanescent field that only penetrates a relatively small thickness of the material. Thus, the main contribution to the detected signal will be made by the effective refractive index at the metal-analyte interface. Though the demonstrated sensitivity of the proposed sensor is rather high and allows label-free detection of biomolecules or biological particles, one should bear in mind that any SP-based sensor is sensitive to all kinds of refractive index variation. Thus, for more reliable and selective measurements, surface functionalization of the plasmonic interface will be required.

The gold nanowire surface can be further modified using appropriate biorecognition components, such as antibodies, aptamers, or ligands, that can selectively recognize cancer-related biomarkers (for example, EpCAM and HER2). Thus, a change in the local refractive index occurs due to the selective interaction with the analyte, resulting in a pronounced shift in the resonance wavelength, which allows for distinguishing these changes from non-target background fluctuations. Moreover, additional methods, such as differential measurement based on reference channels, temperature regulation, and normalization of the buffer, can be utilized to reduce non-selective impacts on the system and achieve high-accuracy measurements. Therefore, such an approach allows one to effectively discriminate target-specific phenomena from refractive index variations

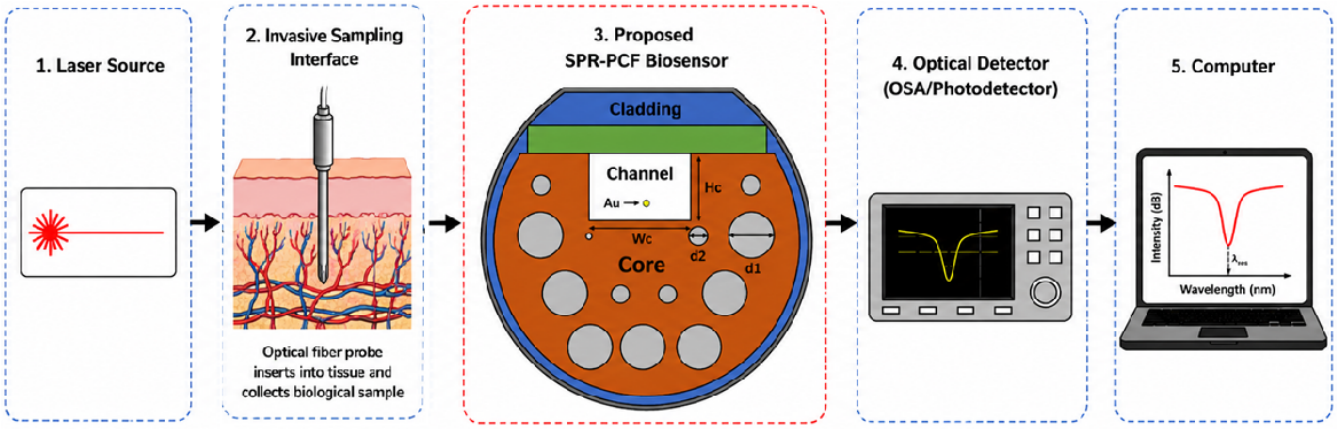

FIGURE 11. Schematic illustration of the experimental setup for the proposed gold nanowire-based quasi D-shaped SPR-PCF biosensor.

caused by the environment. Thus, it can be concluded that the developed sensor is most applicable to the bulk detection of biological samples when the refractive index variations represent cell density alterations or diseases in question. The approach used in the modeling in this study provides a convenient tool for investigating the sensor characteristics. More advanced modeling approaches, including cell-specific interactions, may be suggested in future studies.

3.7. Possible Experimental Validation Procedure

While the current study involves numerical simulations of the FEM type, the proposed SPR-PCF biosensor with integrated nanowires can be experimentally realized through the use of known techniques for the fabrication and characterization of optical structures. The photonic crystal fiber itself can be fabricated via the conventional stack-and-draw technique, which allows for precise manipulation of the air-holes dimensions and core creation. The U-shaped micro-channel next to the core of the fiber can be produced via modern micromachining technologies, such as focused ion beam (FIB) and femtosecond laser ablation, ensuring sub-micrometer accuracy in creating the micro-channel itself. The embedding of the gold nanowire inside the micro-channel can be done via micro-manipulation or capillary-driven self-assembly procedures. While positioning of the nanowire is still challenging from an experimental point of view, recent developments in nanofabrication and micro-positioning ensure its possible realization.

For experimental demonstration, a broadband near-infrared (NIR) light source may be used for injection in the PCF structure, followed by analysis of the output spectrum with the help of an optical spectrum analyzer (OSA), as shown in Fig. 11. It is possible to quantify the wavelength shift due to changes in the refractive index of biological samples, leading to label-free identification of cancer cells. PCF-SPR systems of the described configuration have already been experimentally implemented in previous work, proving their real-life applicability. Moreover, the sensor under consideration is easier to fabricate than multilayer structures, due to the use of one gold nanowire only.

4. CONCLUSION

A gold nanowire incorporated a quasi-D-shaped SPR-PCF biosensor was presented for the extremely sensitive identification of cancer cells in the near-infrared wavelength range. The configuration of localized nanowire has replaced the traditional gold thin film to facilitate confinement loss and phase matching between the core guiding mode and LSPR mode. Optimization of the parameters, such as the diameter of the nanowire, the number of air holes, the pitch, and micro-channel size, has demonstrated remarkable sensing performance. The optimized parameters have demonstrated a maximum wavelength sensitivity of 42857 nm/RIU and an amplitude sensitivity of 189 RIU^{-1} for the refractive index range of 1.36 to 1.40. The nano-wire-based configuration provides better confinement loss peaks and interaction strength to enable accurate sensing. Fabrication feasibility studies demonstrate the possibility of fabrication using conventional PCF fabrication technology. Therefore, the proposed biosensor may serve as an excellent platform for biomedical sensing applications.

REFERENCES

[1] Singh, S., R. Kumar, B. Chaudhary, P. Bhardwaj, V. K. Upaddhyay, A. Upadhyay, and M. G. Daher, "Gold immobilized SPR-Enhanced PCF biosensor for detection of cancer cells: A numerical simulation," *Plasmonics*, Vol. 20, No. 6, 3535–3544, 2025.

[2] Shakya, A. K., A. Ramola, S. Singh, and A. Vidyarthi, "Optimized design of plasmonic biosensor for cancer detection: Core configuration and nobel material coating innovation," *Plasmonics*, Vol. 20, No. 4, 1789–1810, 2025.

[3] Singh, S. and Y. K. Prajapati, "Novel bottom-side polished PCF-based plasmonic biosensor for early detection of hazardous cancerous cells," *IEEE Transactions on NanoBioscience*, Vol. 22, No. 3, 647–654, Jul. 2023.

[4] Mao, Y., F. Ren, D. Zhou, and Y. Li, "Highly sensitive PCF-SPR RI sensor for cancer detection using gold/graphene/Ti3C2Tx-MXene hybrid layer," *Plasmonics*, Vol. 20, No. 4, 2279–2290, 2025.

[5] Bhuyan, A., A. Khamaru, and A. Kumar, "Black phosphorus-based slotted D-shaped PCF SPR sensor for cancer detection," *Plasmonics*, Vol. 20, No. 7, 5201–5213, 2025.

[6] Abbaszadeh, A. and S. Rash-Ahmadi, "A surface plasmon resonance sensor based on photonic crystal fiber composed of magnesium fluoride and graphene layers to detect aqueous solutions," *Optical and Quantum Electronics*, Vol. 56, 915, 2024.

[7] Liu, Q., X. Zhao, Q. Zhang, Z. Xue, Q. Shang, Y. Lu, and W. Yan, "High sensitivity refractive index sensor based on TiO2-Ag double-layer coated photonic crystal fiber," *Plasmonics*, Vol. 20, No. 5, 2419–2432, 2025.

[8] Divya, J., S. Selvendran, A. S. Raja, and V. Borra, "A novel plasmonic sensor based on dual-channel D-shaped photonic crystal fiber for enhanced sensitivity in simultaneous detection of different analytes," *IEEE Transactions on Nanobioscience*, Vol. 23, No. 1, 127–139, Jan. 2024.

[9] Nagavel, B., H. Dagar, and P. Krishnan, "High-performance dual-core bilateral surface optimized PCF SPR biosensor for early detection of six distinct cancer cells," *Plasmonics*, Vol. 20, No. 7, 4799–4809, 2025.

[10] Huraiya, M. A., S. G. Ramaraj, S. M. S. Hossain, K. Chakrabarti, H. Tabata, and S. M. A. Razzak, "A highly optimized and sensitive bowtie shape-based SPR biosensor for different analyte detection," *Nanoscale Advances*, Vol. 7, No. 3, 899–908, 2025.

[11] Singh, S. and V. Kaur, "Photonic crystal fiber sensor based on sensing ring for different blood components: Design and analysis," in *2017 Ninth International Conference on Ubiquitous and Future Networks (ICUFN)*, 399–403, Milan, Italy, 2017.

[12] Kumar, D., J. K. Rakshit, M. P. Singh, C. Nayak, and A. R. Bin, "High-Q photonic crystal-based cascaded concentric microring resonator with topological edge states for cancer detection," *Physics Letters A*, Vol. 564, 131061, 2025.

[13] Ferdous, A. H. M. I., B. Akter, A. Priya, L. M. Leo, R. T. Prabu, B. N. Sathi, D. Kundu, M. G. Sadeque, M. S. Islam, S. H. Ahammad, and A. N. Z. Rashed, "Octagonal PCF with square-core for surface enhanced spectroscopic properties: A new frontier in terahertz chemical sensing," *Plasmonics*, Vol. 19, No. 3, 1257–1268, 2024.

[14] Hamzaoui, A., A. Aouiche, S. Gouder, H. E. Abdellatif, S. A. Khan, and A. Belaadi, "Machine learning-enhanced surface plasmon resonance sensor with D-shaped dual-core photonic crystal fiber design," *Journal of Fluorescence*, Vol. 35, No. 11, 11 409–11 422, 2025.

[15] Ooha, Y., Y. Vasimalla, M. Ravikumar, B. Ramachandran, and S. Kumar, "Highly sensitive surface plasmon resonance sensor utilizing black phosphorus and iron sesquioxide for real-time biomolecule detection," *Plasmonics*, Vol. 20, 10 745–10 762, 2025.

[16] Azab, M. Y., M. F. O. Hameed, A. M. Heikal, M. A. Swillam, and S. S. A. Obayya, "Design considerations of highly efficient D-shaped plasmonic biosensor," *Optical and Quantum Electronics*, Vol. 51, 15, 2019.

[17] Singh, S., B. Chaudhary, A. Upadhyay, D. Sharma, N. Ayyanar, and S. A. Taya, "A review on various sensing prospects of SPR based photonic crystal fibers," *Photonics and Nanostructures — Fundamentals and Applications*, Vol. 54, 101119, 2023.

[18] Sardar, M. R. and M. Faisal, "Dual-core dual-polished PCF-SPR sensor for cancer cell detection," *IEEE Sensors Journal*, Vol. 24, No. 7, 9843–9854, Apr. 2024.

[19] Abdullah, H., M. S. Uddin, and B. K. Paul, "High-sensitivity gold-coated refractive index biosensor based on surface plasmon resonance," *Plasmonics*, Vol. 18, No. 6, 2213–2223, 2023.

[20] Shahbazlou, S. V., S. Vandghanooni, B. Dabirmanesh, M. Eskandani, and S. Hasannia, "Recent advances in surface plasmon resonance for the detection of ovarian cancer biomarkers: A thorough review," *Microchimica Acta*, Vol. 191, No. 11, 659, 2024.

[21] Sayem, M. A., T. Ahmed, M. A. A.-M. Pinto, and M. F. Hossain, "Plasmonic sensor for detecting high refractive index with analyte-infused photonic crystal fiber," in *2023 26th International Conference on Computer and Information Technology (ICCIT)*, 1–5, Cox's Bazar, Bangladesh, Dec. 2023.

[22] Chowdhury, A. A., M. R. H. Khan, M. R. Islam, A. N. M. Iftekher, M. S. Hosen, M. H. Mim, and M. M. Nishat, "Gold nanowire-infused square-clad SPR-PCF biosensor for detection of various cancer cells," *Sensing and Bio-Sensing Research*, Vol. 45, 100670, 2024.

[23] Khodatars Dashtmian, M. R., V. Fallahi, M. Seifouri, and S. Olyaee, "Gold nanowire-enhanced SPR-PCF biosensor for high-throughput cancer cell detection in near-infrared," *Plasmonics*, Vol. 20, 11 853–11 865, 2025.

[24] Ramola, A., S. Singh, and A. Marwaha, "Modelling and parameter quantification of plasmonic sensor based on external sensing for analysis of body liquids," *Biosensors and Bioelectronics: X*, Vol. 14, 100358, Sep. 2023.

[25] Ramola, A., A. K. Shakya, and A. Bergman, "Comprehensive analysis of advancement in optical biosensing techniques for early detection of cancerous cells," *Biosensors*, Vol. 15, No. 5, 292, May 2025.

[26] Ramola, A., A. K. Shakya, and A. Bergman, "Finite element method-based modeling of a novel square photonic crystal fiber surface plasmon resonance sensor with a Au-TiO2 interface and the relevance of artificial intelligence techniques in sensor optimization," *Photonics*, Vol. 12, No. 6, 565, Jun. 2025.

[27] Ramola, A., A. K. Shakya, A. Droby, and A. Bergman, "Numerical study of a novel Kagome-inspired photonic crystal fiber-based surface plasmon resonance biosensor for detection of blood components and analytical targets," *Biosensors*, Vol. 15, No. 8, 539, Aug. 2025.

[28] Ramola, A., A. K. Shakya, V. Kumar, and A. Bergman, "Recent advances in photonic crystal fiber-based SPR biosensors: design strategies, plasmonic materials, and applications," *Micromachines*, Vol. 16, No. 7, 747, Jun. 2025.

[29] Ramola, A., A. K. Shakya, N. Balal, and A. Bergman, "Theoretical investigation of early cancer biomarker sensing using a PMMA-gold hybrid quasi-D-shaped photonic-crystal-fiber-based surface plasmon resonance biosensor," *Micromachines*, Vol. 17, No. 1, 68, 2026.

[30] Yin, Z., J. Wang, X. Zhang, X. Jing, and S. Li, "Triple-channel SPR ion-imprinted fiber sensor enabled by MoS2 thickness-tuned resonance for multiplexed heavy metal ion detection," *Optics Letters*, Vol. 50, No. 24, 7596–7599, Dec. 2025.

[31] Yin, Z., X. Jing, and S. Li, "High-sensitivity parallel SPR probes for refractive index and temperature sensing," *Infrared Physics & Technology*, Vol. 150, 106036, 2025.